Complementary Metal Oxide Semiconductor Cantilever Arrays on a Single Chip: Mass-Sensitive Detection of Volatile Organic Compounds

ARTICLE *in* ANALYTICAL CHEMISTRY · AUGUST 2002

Impact Factor: 5.64 · DOI: 10.1021/ac011269j · Source: PubMed

5 AUTHORS, INCLUDING:

Christoph Hagleitner
IBM
102 PUBLICATIONS **1,735** CITATIONS
SEE PROFILE

Andreas Hierlemann
ETH Zurich
290 PUBLICATIONS **4,834** CITATIONS
SEE PROFILE

Anal. Chem. **2002,** *74,* 3084−3095

Complementary Metal Oxide Semiconductor Cantilever Arrays on a Single Chip: Mass-Sensitive Detection of Volatile Organic Compounds

Dirk Lange, Christoph Hagleitner, Andreas Hierlemann,* Oliver Brand, and Henry Baltes

ETH Zurich, Physical Electronics Laboratory, HPT-H4.2, 8093 Zurich, Switzerland

The sensing behavior of polymer-coated resonant cantilevers for mass-sensitive detection of volatile organic compounds was investigated. Industrial complementary metal oxide semiconductor (CMOS) technology combined with subsequent CMOS-compatible micromachining was used to fabricate a single-chip system comprising the transducers and all necessary driving and signal-conditioning circuitry. An analytical model was developed to describe the mass-sensing mechanism of polymer-coated resonant cantilevers. The model was validated by measurements of various gaseous analytes. As an exemplary application, the quantitative analysis of a binary mixture using an array of four cantilevers is described. Experimental results are given for the concentration prediction of a mixture of *n*-octane and toluene. Finally, it was established that the limit of detection achieved with cantilever sensors is comparable to that of other acoustic wave-based gas sensors.

Micromachined cantilevers commonly employed in atomic force microscopy (AFM)[1] have been proposed to measure a variety of different quantities, such as, temperature,[2] magnetic fields,[3] and viscosity.[4] The cantilever deflection can be used to assess surface stress changes upon absorption of a species.[5,6] Cantilevers also constitute a promising type of mass-sensitive transducer for chemical sensing. The cantilever base is firmly attached to the silicon support. The free-standing cantilever end is coated with a sensitive layer, which, for example, absorbs analyte molecules from the gas phase. There are two fundamentally different operation methods: (a) static mode, measurement of the cantilever deflection upon stress changes or mass loading by means of, for example, a laser;[5−9] (b) dynamic mode, excitation of the cantilever in its fundamental vibration mode and measurement of the change in resonance frequency upon mass loading[6,10−13] in analogy to other mass-sensitive devices.[14−18] The two methods impose completely different constraints on the cantilever design for optimum sensitivity. Method a requires long and soft cantilevers to achieve large deflections, whereas method b requires short and stiff cantilevers to achieve high operation frequencies. Method b is preferable with regard to integration of electronics and simplicity of the setup (self-excitation using amplifying feedback loop).[6,10−13,19] Method a can be applied in liquids as well,[5,6,13] which is rather difficult using the dynamic mode. The excitation of the cantilever in the resonant mode is usually performed by applying piezoelectric materials (ZnO)[19] or by making use of the bimorph effect, i.e., the different temperature coefficients or mechanical stress coefficients of the various layer materials forming the cantilever.[6−13] This difference in material properties gives rise to a cantilever deflection upon heating or applying mechanical forces. Periodic heating pulses in the cantilever base thus can be used to thermally excite the cantilever in its resonance mode at 10−500 kHz.[10−12] The detection of the frequency changes can be done by embedding piezoresistors in the cantilever base,[6,10−13] by measuring motional capacitance changes,[20] or by using optical detection by means of a laser.[5,8,9,21−23] The mass resolution of the cantilevers is in the range of a few picograms.[5,8−12,24] Chemical sensor applications of resonant cantilevers and bridge structures

* Corresponding author. E-mail: hierlema@iqe.phys.ethz.ch. Phone: ++41 1 633 3494. Fax: ++41 1 633 1054.

(1) Berger, R.; Gerber, Ch.; Lang, H. P.; Gimzewski, J. *J. Microelectron. Eng.* **1997**, *35*, 375−379.
(2) Barnes, J. R.; Stephenson, R. J.; Welland, M. E.; Gerber, Ch.; Gimzewski, J. K. *Nature* **1994**, *372*, 79−81.
(3) Leichlé, T. C.; von Arx, M.; Allen, M. G. *Proc. IEEE MEMS 2001*, Interlaken, Switzerland, 2001; pp 274−277.
(4) Oden, P. I.; Chen, G. Y.; Steele, R. A.; Warmack, R. J.; Thundat, T. *Appl. Phys. Lett.* **1996**, *68*, 3814−3816.
(5) Fritz, J.; Baller, M. K.; Lang, H. P.; Rothuizen, H.; Vettiger, P.; Meyer E.; Güntherodt H. J.; Gerber, Ch.; Gimzewski J. K. *Science* **2000**, *288*, 316−318.
(6) Boisen, A.; Thaysen, J.; Jesenius, H.; Hansen, O. *Ultramicroscopy* **2000**, *82*, 11−16.
(7) Lang, H. P.; Baller, M. K.; Berger, R.; Gerber, C.; Gimzewski, J. K.; Battiston, F.; Fornaro, P.; Ramseyer, J. P.; Meyer, E.; Güntherodt, H. J. *Anal. Chim. Acta* **1999**, *393*, 59−65.
(8) Gimzewski, J. K.; Gerber, C.; Meyer, E.; Schlittler, E. E. *Chem. Phys. Lett.* **1994**, *217*, 589−594.
(9) Berger, R.; Delamarche, E.; Lang, H. P.; Gerber, C.; Gimzewski, J. K.; Meyer, E.; Güntherodt, H. J. *Science* **1997**, *276*, 2021.
(10) Baltes, H.; Lange, D.; Koll, A. *IEEE Spectrum* **1998**, *9*, 35−38.
(11) Hierlemann, A.; Lange, D.; Hagleitner, C.; Kerness, N.; Koll, A.; Brand O.; Baltes, H. *Sens. Actuators, B* **2000**, *70*, 2−11.
(12) Lange, D.; Hagleitner, C.; Brand, O.; Baltes, H. *Digest of Technical Papers TRANSDUCERS 1999*, Sendai, Japan, 1999; pp 1020−1023.
(13) Jesenius, H.; Thaysen, J.; Rasmussen, A. A.; Veje, L. H.; Hansen, O.; Boisen, A. *Appl. Phys. Lett.* **2000**, *76*, 2615−2617.
(14) King, W. H. *Anal. Chem.* **1964**, *36*, 206−222.
(15) Nieuwenhuizen, M. S.; Venema, A. *Sens. Mater.* **1989**, *5*, 261−300.
(16) Grate, J. W.; Martin, S. J.; White, R. M. *Anal. Chem.* **1993**, *65*, 940A−948A, 987A−996A.
(17) Bodenhöfer, K.; Hierlemann, A.; Noetzel, G.; Weimar, U.; Göpel, W. *Anal. Chem.* **1996**, *68*, 2210.
(18) Martin, S. J.; Frye, G. C.; Spates, J. J.; Butler, M. A. *Proc. IEEE Ultrason. Symp.* **1996**, 423−433.
(19) Lee, S. S.; White, R. M. *Sens. Actuators, A* **1996**, *52*, 41−45.

10.1021/ac011269j CCC: $22.00
Published on Web 05/18/2002

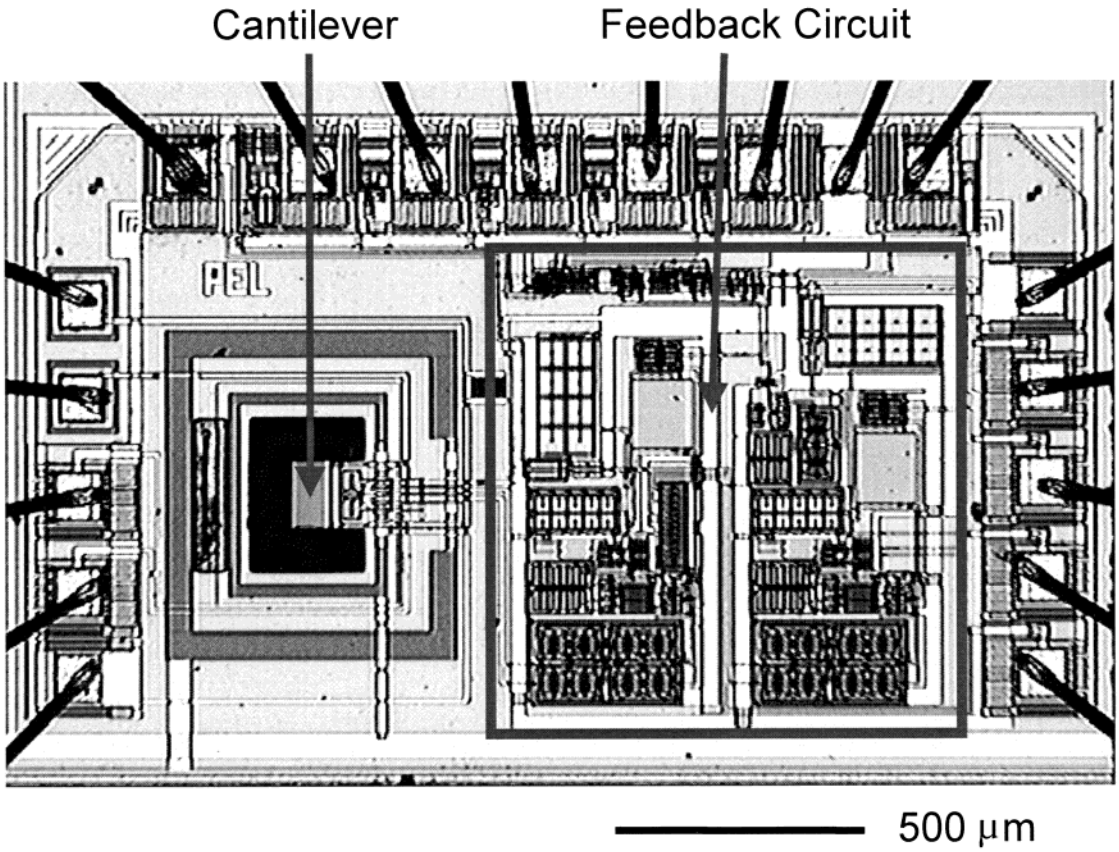

Figure 1. Micrograph of a 150-μm-long resonant cantilever and the on-chip feedback circuit.

include humidity sensors[24,25] or the detection of mercury vapors.[26] Complementary metal oxide semiconductor (CMOS) cantilevers coated with chemically sensitive polymers have previously been used for the detection of volatile organic compounds.[11,12,23,24,27,28] A miniaturized system with an array of coated cantilevers for the simultaneous detection of hydrogen and mercury vapors was reported in ref 29. Quantitative detection of the components of a binary mixture was demonstrated by our group and by Kim et al.[30] Cantilevers can be included in application-specific chemical sensor systems[11] along with other types of CMOS-based microtransducers such as capacitors[31,32] or microcalorimeters.[33]

The cantilever in this paper is operated in the dynamic mode, and the change of the resonance frequency upon mass-loading is measured. The operation features of resonant cantilevers are, as already mentioned, similar to those of other well-established mass sensitive gas sensors such as thickness shear mode resonators (TSMR, quartz microbalances)[14−17] and surface acoustic (SAW)[16−18] devices. For an overview on micromachined resonant sensors see ref 35. Cantilever fabrication using CMOS-compatible micromachining and the design of a single-chip system comprising a cantilever sensor and the corresponding readout circuitry will be detailed below. A model for the mass-sensitive detection of gaseous species will be developed and confirmed by experimental results. The use of cantilever arrays for discrimination of analytes in mixtures will be demonstrated, and the performance of such resonant cantilever gas sensors will be compared to those of thickness shear mode resonators (TSMR) and surface acoustic wave (SAW) devices.

System Design. The mass-sensitive chemical sensor system is a single-chip system comprising a cantilever-type transducer operated in the resonant mode and dedicated feedback circuitry on the same substrate (Figure 1). The cantilever consists of single-crystal silicon covered by dielectric layers such as silicon oxide

(20) Britton, C. L.; Warmack, R. J.; Smith, S. F.; Oden, P. I.; Jones, R. L.; Thundat, T.; Brown, G. M.; Bryan, W. L.; DePriest, J. C.; Ericson M. N.; Emery, M. S.; Moore, M. R.; Turner, G. W.; Wintenberg, A. L.; Threatt, T. D.; Hu, Z.; Clonts, G.; Rochelle, J. M. *Proceedings 20th Anniversary Conference on Advanced Research in VLSI. IEEE Comput. Soc.* Los Alamitos, CA, 1999; pp 359−68.
(21) Wachter, E. A.; Thundat, T. *Rev. Sci. Instrum.* **1995**, *66*, 3662−3667.
(22) Lang, H. P.; Berger, R.; Battiston, F.; Ramseyer J. P.; Meyer E.; Andreoli C.; Brugger J.; Vettiger P.; Despont, M.; Mezzacasa, T.; Scandella, L.; Güntherodt, H. J.; Gerber, C.; Gimzewski, J. K. *Appl. Phys. A* **1998**, *66*, 161−64.
(23) Maute, M.; Raible, S.; Prins, F. E.; Kern, D. P.; Ulmer, H.; Weimar, U.; Göpel, W. *Sens. Actuators, B* **1999**, *58*, 505−511.
(24) Thundat, T.; Chen, G. Y.; Warmack, R. J.; Allison, D. P.; Wachter, E. A. *Anal. Chem.* **1995**, *67*, 519−521.
(25) Boltshauser, T.; Schönholzer, M.; Brand, O.; Baltes, H. *J. Micromech. Microeng.* **1992**, *2*, 205−207.
(26) Thundat, T.; Wachter, E. A.; Sharp, S. L.; Warmack, R. J. *Appl. Phys. Lett.* **1995**, *66*, 1695−1697.
(27) Lange, D.; Koll, A.; Brand, O.; Baltes, H. *Proc. SPIE* **1998**, *3224*, 233−243.
(28) Lange, D.; Hagleitner, C.; Brand, O.; Baltes, H. *Proc. IEEE MEMS 2000*, Myazaki, Japan, 2000; pp 547−552.
(29) Britton, C. L.; Jones, R. L.; Oden, P. I.; Hu, Z.; Warmack, R. J.; Smith, S. F.; Bryan, W. L.; Rochelle, J. M. *Ultramicroscopy* **2000**, *82*, 17−21.
(30) Kim, B. H.; Prins, F. E.; Kern, D. P.; Raible, S.; Weimar, U. *Sens. Actuators, B* **2001**, *78*, 12−18.
(31) Koll, A.; Kummer, A.; Brand, O.; Baltes, H. *Proc. SPIE* **1999**, *3673*.
(32) Hagleitner, C.; Koll, A.; Vogt, R.; Brand, O.; Baltes, H. *Technical Digest TRANSDUCERS 1999*, Sendai, Japan, 1999; pp 1012−1015.
(33) Kerness, N.; Koll, A.; Schaufelbühl, A.; Hagleitner, C.; Hierlemann, A.; Brand, O.; Baltes, H.*Proc. IEEE MEMS* 2000, Myazaki, Japan, 2000; pp 96−101.
(34) Baltes, H.;Paul, O.; Brand, O. *Proc. IEEE* **1998**, *86*, 1660−1678.

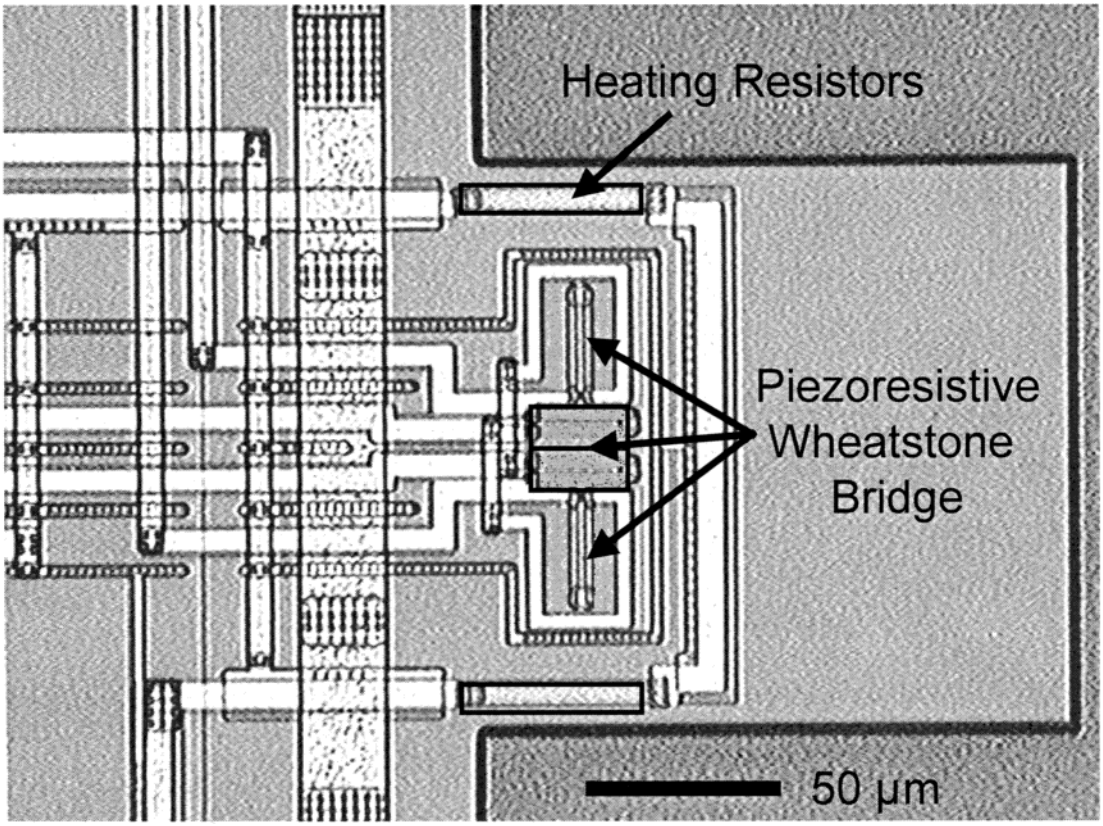

Figure 2. Closeup of a 150-μm-long resonant cantilever. Four piezoresistors, each of which comprises two "subresistors", form a Wheatstone bridge. The two heating resistors for symmetric thermal actuation of the cantilever are also marked.

or silicon nitride for electrical insulation of the integrated electronic components. A closeup view is shown in Figure 2. The cantilever is vibrated using thermal actuation; i.e., two heating resistors integrated in the cantilever base are heated periodically. The temperature increase on the cantilever generates a bending moment due to the difference in thermal expansion coefficients of the silicon and the covering dielectric layers (thermal bimorph effect). The area of periodic temperature variation is closely confined to the region around the heaters due to the high excitation frequency of ~400 kHz. At frequencies higher than the corner frequency of ~1 kHz (speed of the thermal equilibration processes in the cantilever), the efficiency of the thermal actuation usually significantly drops. However, the created bending moment is still sufficient to cause harmonic transverse vibrations of the cantilever with an amplitude of a few nanometers. The cantilever vibrations are detected by piezoresistors arranged in a Wheatstone bridge configuration. The Wheatstone bridge delivers an output voltage upon mechanical deformation of the piezoresistors, which are located in the cantilever base region (Figure 2).

The cantilever constitutes the frequency-determining element of an oscillator circuit, as is illustrated in the block diagram of the sensor system in Figure 3. The output signal of the piezoresistive Wheatstone bridge is amplified in two stages and high-pass filtered between the amplification stages. A comparator limits the resulting square-wave-shaped signal. The feedback loop is then closed via an inverter with a Schmitt trigger operated as a delay

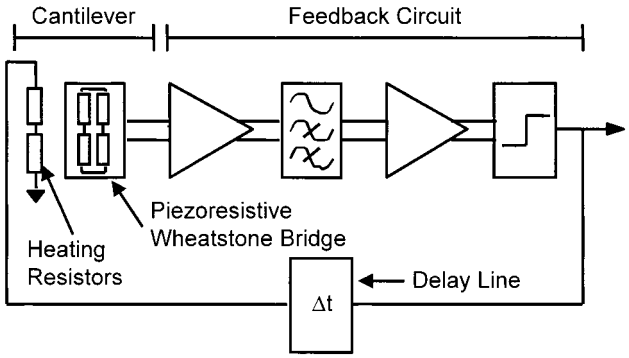

Figure 3. Block diagram of the resonant beam gas sensor system.

element. The rise time of the Schmitt trigger is controlled by an externally applied loading current. This way, the phase shift is adjusted to ensure positive feedback. To close the feedback loop, an actuation signal is generated that triggers the heating resistors on the cantilever. The result is an integrated oscillator operating at the cantilever resonance frequency with a short-term frequency stability better than 0.1 Hz. The integration of the feedback loop on chip massively improves the signal-to-noise characteristics of the sensor. The detection of mass changes of less than 1 pg on the cantilever was achieved by recording the corresponding shifts in the cantilever resonance frequency.

To operate the oscillator, the generated displacement and, hence, the heating pulses have to be on the same frequency order as the excitation voltage. This is solved by superimposing a static dc offset on the periodic excitation voltage. The intended periodic

(35) Brand, O.; Baltes, H. Micromachined resonant sensors. In *Sensors Update*; Baltes, H., Göpel, W., Hesse, J., Eds.; VCH: Weinheim, Germany, 1998; Vol. 4, p 36.

temperature fluctuation is accompanied by a general temperature increase on the cantilever, which results from the unavoidable static component of the heating power. The power dissipation in the piezoresistors of the Wheatstone bridge constitutes a second source of heating. Both heating effects can cause a total temperature increase of up to 19 °C above ambient temperature in the chemically sensitive region of the cantilever. The temperature increase is ~3 °C above ambient temperature at routine operation.

Fabrication. The resonant cantilever sensors were fabricated using an industrial 0.8-μm double-metal CMOS process of Austriamicrosystems (Graz, Austria), in combination with micromachining postprocessing steps.[34] The fabrication process flow is detailed in ref 27. The CMOS-based sensor production relies on established IC processes and offers the crucial advantage of cointegrating even several different transducers with signal-conditioning or -processing circuitry on the same sensor chip. After completion of the CMOS process, the cantilevers are formed in two postprocessing steps. First, silicon membranes are created by anisotropic silicon backside etching with KOH in combination with an electrochemical etch stop at the n-well (The n-well was created by implantation during the CMOS process). To this end, a silicon nitride layer is deposited on the backside of the wafer, and the etch windows for the anisotropic etching are defined. During the etching step, the wafer front is not exposed to the KOH solution so that the metal connections of the circuits cannot be damaged. In the second postprocessing step, cantilevers are released by opening the silicon membrane around the designated cantilever shape using frontside reactive ion etching (RIE). The resulting cantilevers consist of the silicon n-well covered by the dielectric layers of the CMOS process (silicon nitride, silicon oxide). The resonance frequency of the uncoated 150-μm-long cantilevers is 350−390 kHz with a quality factor of 950 in air. The quality factor of the resonant silicon cantilevers at atmospheric pressure is dominated by the viscous damping in the surrounding air. In comparison to cantilevers employed in scanning probe microscopy (SPM), the cantilevers investigated in this work exhibit high quality factors. This is partly because the cantilevers are not operated in close vicinity to a sample surface, and hence, no squeezed-film damping occurs. The distance to the bottom of the etch cavity is 380 μm, i.e., large in comparison to the cantilever dimensions. Furthermore, the quality factor is a function not only of the resonance frequency but also of the cantilever geometry and its spring constant.[36] While SPM cantilevers for dynamic mode operation typically exhibit spring constants between 1 and 40 N/m, the cantilevers in this study were designed to exhibit a much higher spring constant of 800 N/m. As can be seen from Figure 4, the measured quality factor of cantilevers in fundamental resonance strongly increases with increasing resonance frequency up to 200 kHz, reaching maximum values of ~1000. This behavior is predicted by the theory of a damped harmonic cantilever beam with a damping term proportional to the beam velocity.[37] A theoretical estimation of the actual quality factors would, however, require a model for the dependence of the damping term on the cantilever dimensions. At frequencies higher than 200 kHz, a saturation-like behavior of the quality factor has been observed, indicating additional loss mechanisms, such as coupling losses into higher resonant modes or losses due to onset of acoustic radiation at higher frequencies.

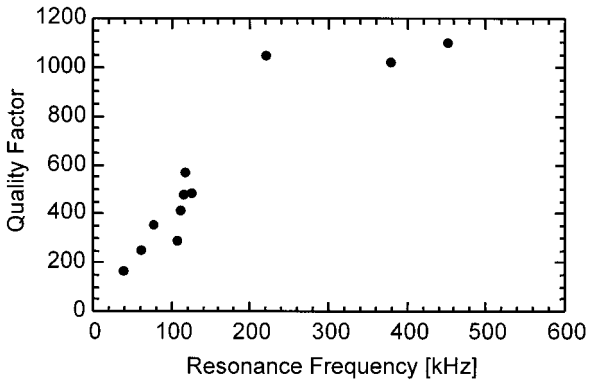

Figure 4. Experimentally determined quality factors of various cantilevers operating in air (10^5 Pa) at different frequencies (different cantilever geometry).

In a last step, the cantilevers are spray-coated with various polymers, which act as chemically sensitive layers.

Mass-Sensitive Behavior. Polymers deposited on the cantilevers serve as sensitive films to detect volatile organic compounds in air. We have restricted our investigations to polymeric films for which physisorption and bulk dissolution of the analyte within the polymer volume are the predominant mechanisms. Upon absorption of analytes by the coating, the physical properties of the polymer film, such as its mass, change. This mass change is detected by monitoring the corresponding resonance frequency shift of the coated cantilever upon analyte exposure.

The partition coefficient K_c characterizes the absorption behavior of a polymer with regard to different volatile species.[38] It is a chemical equilibrium constant and is defined as the ratio of analyte concentration in the gas phase c_A (μg/L) and analyte concentration in the polymeric phase c_{Poly} (μg/L):

$$K_c = c_{Poly}/c_A \tag{1}$$

The partition coefficient, K_c, strongly depends on the nature of polymer and analyte, the analyte saturation vapor pressure, and the operation temperature.

When an analyte is absorbed in the polymeric film, the mass change produces a frequency change of the resonant cantilever, which is essentially functioning as a balance. A schematic of the transducer is shown in Figure 5. A silicon cantilever of thickness $t_{Si} = 5.5-6$ μm is covered with silicon dioxide layers ($t_{Ox} = 2.4$ μm) and a silicon nitride passivation ($t_{Ni} = 1.1$ μm). The silicon nitride passivation protects embedded electrical components. The cantilever is coated with a polymer layer, which is between 1 and 10 μm thick (t_L). The fundamental resonance frequency of the composite beam for small deflections is given by[39,40]

$$f_0 = \frac{{\lambda_0}^2}{2\pi L^2}\sqrt{\frac{\hat{E}_{Si}I_{Si} + \hat{E}_{Ox}I_{Ox} + \hat{E}_{Ni}I_{Ni} + \hat{E}_{L}I_{L}}{\rho_{mean}F}} \tag{2}$$

Here, $\hat{E}$ denotes the apparent Young's modulus of each material,

(36) Blom, F. R.; Bouwstra, S.; Elwenspoek, M.; Fluitman, J. H.; *J. Vac. Sci. Technol. B* **1992**, *10*, 19−26.

(37) Buser, R.A. Resonant Sensors. In *Sensors, A Comprehensive Survey*; Bau, H. H., de Rooij, N. F., Kloeck, B., Eds.; VCH: Weinheim 1994; Vol. 7, pp 205−284.

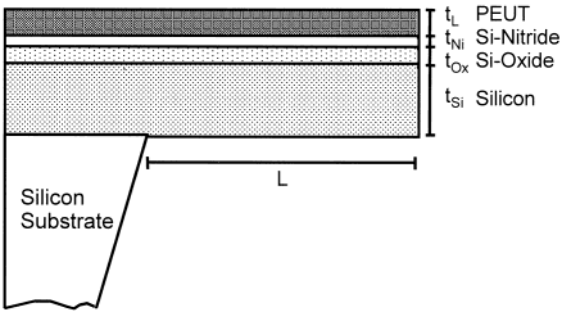

Figure 5. Cross section of the composite cantilever beam.

I is the respective moment of inertia, and ρ_{mean} is the average specific mass density of the composite beam. F denotes the cross-sectional area, and L denotes the length of the cantilever. λ_0 is an integration constant and has a value of 1.875 for the cantilever materials and geometry under consideration.

The moment-of-inertia contribution of each layer depends on the distance of the particular layer to the neutral layer of the beam. The neutral layer is a particular plane of the beam where the internal mechanical stress during vibration equals zero. When the beam shown in Figure 5 bends upward, the uppermost layers experience compressive stress due to the cantilever bending, whereas the bottom layers experience tensile stress. The opposite holds true when the cantilever bends downward. The neutral layer is the plane near the cantilever center, which experiences neither tensile nor compressive stress during oscillation though it is deformed through the cantilever motion. The position, h_n, of this neutral layer was determined to be[40]

$$h_n = \frac{1}{2(\hat{E}_{Si}t_{Si} + \hat{E}_{Ox}t_{Ox} + \hat{E}_{Ni}t_{Ni} + \hat{E}_L t_L)} \times \{\hat{E}_{Si}t_{Si}^2 + \hat{E}_{Ox}[(t_{Si} + t_{Ox})^2 - t_{Si}^2] + \hat{E}_{Ni}[(t_{Si} + t_{Ox} + t_{Ni})^2 - (t_{Si} + t_{Ox})^2] + \hat{E}_L[h^2 - (h - t_L)^2]\} \quad (3)$$

where h is the total thickness of the cantilever, i.e., $h = t_{Si} + t_{Ox} + t_{Ni} + t_L$. Starting from the neutral layer position h_n, the individual moments of inertia of the four cantilever layers can be determined:

$$I_{Si} = (b/3)[h_n^3 - (h_n - t_{Si})^3]$$
$$I_{Ox} = (b/3)[(h_n - t_{Si})^3 - (h_n - t_{Si} - t_{Ox})^3]$$
$$I_{Ni} = (b/3)[(h_n - t_{Si} - t_{Ox})^3 - (h_n - t_{Si} - t_{Ox} - t_{Ni})^3]$$
$$I_L = (b/3)[(h_n - t_{Si} - t_{Ox} - t_{Ni})^3 - (h_n - h)^3] \quad (4)$$

The average specific mass density (cantilever materials and sensitive layer), ρ_{mean}, and the cantilever mass density (only cantilever sandwich materials), ρ_{cant}, are

$$\rho_{mean} = \frac{\rho_{Si}t_{Si} + \rho_{Ox}t_{Ox} + \rho_{Ni}t_{Ni} + \rho_L t_L}{t_{Si} + t_{Ox} + t_{Ni} + t_L}$$
$$\rho_{cant} = \frac{\rho_{Si}t_{Si} + \rho_{Ox}t_{Ox} + \rho_{Ni}t_{Ni}}{t_{Si} + t_{Ox}\, t_{Ni}} \quad (5)$$

Inserting eqs 4 and eq 5 into eq 2 yields the resonance frequency of the composite beam.

Additional mass on the cantilever leads to a decrease in the resonance frequency. Therefore, negative resonance frequency shifts are detected upon absorption of a gaseous analyte in the polymer. These frequency shifts originate from the polymer mass density increase ρ_L as a consequence of the additional mass of the absorbed gas molecules.

Due to the high spring constant of the cantilever ($k \approx 800$ N/m), influences from changes in the elastic properties of the polymer upon gas absorption, the effects of which are more than 2 orders of magnitude smaller, can be neglected. Under the assumption that the cantilever is covered with a polymer layer of uniform thickness, the average mass density (ρ_{mean}) change of the cantilever as a consequence of the polymer density change (polymer swelling can be neglected in a first-order approximation at such low analyte concentrations[17]) is given by

$$\frac{\partial \rho_{mean}}{\partial \rho_L} = \frac{t_L}{t_{Si} + t_{Ox} + t_{Ni} + t_L} = \frac{t_L}{h} \quad (6)$$

Starting from eq 2, the shift of the resonance frequency, f_0, caused by a change in the mass density of the polymer layer can be calculated:

$$G = \partial f_0/\partial \rho_L = \frac{\partial f_0}{\partial \rho_{mean}} \frac{\partial \rho_{mean}}{\partial \rho_L} = -\frac{1}{2}\frac{f_0}{\rho_{mean}}\frac{t_L}{h} \quad (7)$$

Here, G represents the gravimetric sensitivity, i.e., the change in frequency due to a change in polymer density. The corresponding mass sensitivity $G_m = GV_L$ is determined by taking into account the polymer volume V_L.

The origin of the polymer density change $\partial\rho_L$ is the absorption of the analyte gas of concentration c_A. A cantilever resonance frequency shift indicates the corresponding mass change. The sensitivity, S, of the resonant gas sensor is defined as

$$S = \partial f_0/\partial c_A \quad (8)$$

As demonstrated earlier, the resonance frequency change results from the polymer density change upon analyte absorption:

$$S = (\partial f_0/\partial \rho_L)(\partial \rho_L/\partial c_A) = GS_A \quad (9)$$

(38) Grate, J.W.; Abraham, M. H. *Sens. Actuators, B* **1991**, *3*, 85−111.
(39) Weaver, W.; Timoshenko; S. P.; Young, D. H. *Vibration Problems in Engineering*; Wiley: New York, 1990.
(40) Gere, J. M.; Timoshenko, S. P. *Mechanics of Materials*, 3rd ed.; PWS: Kent, U.K., 1990.

G describes the mechanical properties of the cantilever device, whereas S_A relates to the polymer/analyte interactions. The mass increase, ∂m_L, of the polymer with volume, V_L, and the corresponding polymer density increase, $\partial \rho_L$, upon an analyte concentration change, ∂c_A, is given by

$$\partial \rho_L = \partial m_L / V_L = K_c \partial c_A \tag{10}$$

The analyte sensitivity, S_A, hence equals the partition coefficient, K_c, when mass concentrations (mass/volume) are used. Finally, the sensitivity, S (Hz/(μg/L)), of the cantilever gas sensor can be rewritten as

$$S = -\frac{1}{2} \frac{f_0}{\rho_{mean}} \frac{t_L}{h} K_c \tag{11}$$

EXPERIMENTAL SECTION

Layer Deposition. After completion of the post-CMOS micromachining steps, polymeric films are deposited onto the sensing structures by spray coating with an airbrush (Badger, model 200-F) and shadow masks. A wide range of partial selectivities and sorption properties can be covered by careful selection of the polymeric coating materials. The microsensors investigated were coated with a slightly polar poly(etherurethane) film (PEUT, Thermedics Inc., Woburn, MA) a nonpolar poly(dimethylsiloxane) (PDMS, ABCR, Karlsruhe, Germany), and a strongly polar poly(cyanopropylmethylsiloxane) (PCPMS, ABCR, Karlsruhe, Germany). For spraying, the polymers are dissolved in dichloromethane (concentrations between 0.6 and 3.5 mg/mL). With the exception of PCPMS, the polymers form smooth layers on the transducers after curing.

Gas Tests. For gas tests, dual-in-line packages containing the CMOS gas sensors are mounted in the measurement chamber of a computer-controlled gas manifold. Vapors are generated from specifically developed temperature-controlled (T = 223−293 K) vaporizers, using synthetic air as carrier gas, and then diluted as desired using computer-driven mass-flow controllers. The internal volume of these vaporizers, which distribute the liquid over a large-area packed-bed-type support to maximize surface/volume ratio, is dramatically smaller than that of typical gas-washing bottles ("bubblers").[41] By using these vaporizers, the noise in the sensor signals caused by concentration fluctuations or aerosol formation of the liquid analytes is reduced, and the reproducibility of the adjusted gas-phase concentrations is significantly enhanced. A photoacoustic detector (infrared light excitation) as provided by Innova Airtec Systems is used as an independent reference to assess the actual analyte gas-phase concentrations. The vapor-phase concentrations at the respective temperatures can be calculated following the Antoine equation.[42] All vapors are mixed and temperature-stabilized before entering the thermoregulated chamber. All gas tubings in the manifold are made of stainless steel. The sensors were mounted inside a flow-through cell, and the measurements were performed at a temperature of 301 K. The thermostat used for the measuring chamber was a microprocessor-controlled Julabo FP 30 MH (Julabo, Seelbach, Germany). The gas flow rate to the sensors is 200 mL/min at a total pressure of 10^5 Pa. The response time of the sensors is on the order of seconds. It takes, however, ~5 min (t_{90} = 120 s) to reach an equilibrium state in the setup. This time span is needed to achieve a constant gas concentration (steady state) in the chamber at the chosen flow rate. Typical experiments consisted of alternating exposures to air and vapor. Exposure times of 10−15 min are followed by 10−15 min purging of the chamber with synthetic air. To test for reproducibility, analyte concentrations are ramped up and down.The resonance frequency of the cantilevers is continuously measured using a frequency counter with a gate time of 1 s.

RESULTS AND DISCUSSION

Polymer Influence on Resonance Frequency and Quality Factor. Since the cantilever beam shows a decrease in resonance frequency due not only to the absorption of an analyte in the sensitive layer but also to the deposition of the sensitive layer itself, the polymer thickness can be monitored during the coating procedure. As can be anticipated, the polymer coating leads to a decrease of the vibrational amplitude and to a reduction of the quality factor.

Equation 2 describes the resonance frequency of a composite cantilever beam, one layer of which consists of the deposited polymer. The moments of inertia in eqs 4 and the mean density of the cantilever in eqs 5 are both functions of the polymer thickness. Therefore, eq 2 also describes the dependence of the cantilever resonance frequency on the deposited polymer thickness. Figure 6a shows the measurement results compared to the analytical model for the resonance frequency as a function of the polymer thickness. The polymer thickness is determined using a white-light spectrometer (Axiospeed from Zeiss, Jena, Germany). As can be seen, experimental and theoretical values are in good agreement. It should be noted that a linear model for the decrease of the resonance frequency with increasing polymer thickness is not valid for a thickness of more than 1 μm (modulus contributions). With increasing thickness, the decrease of the cantilever resonance frequency is less than proportional. In fact, for thicknesses above 30 μm, the resonance frequency would increase again, since the system has now changed from a polymer-loaded silicon cantilever to a silicon-loaded polymeric cantilever with the consequence that the resonance frequency again increases linearly with increasing polymer thickness.

Variations in the material properties of the polymer barely influence the cantilever resonance frequency in the investigated range, because the overall elastic properties are dominated by the CMOS materials. As an example, a 50% inaccuracy of the elastic modulus of 100 MPa at a polymer layer thickness of 12 μm results in a variation of the modeled resonance frequency of only 0.8%. The influence of the polymer density is larger but still not significant. Here, an uncertainty of 10% leads to a variation of 1.9%.

Not only is the resonance frequency affected by the polymer thickness but the vibration amplitude and the quality factor are also, as shown in Figure 6b). This is partly due to the fact that quality factor and vibrational amplitude depend to a critical extent on the plastic or viscous properties of the thin polymer films. Furthermore, it is observed that quality factor and amplitude

(41) Bodenhöfer, K.; Hierlemann, A.; Schlunk, R.; Göpel, W. *Sens. Actuators, B* **1997**, *45*/3, 259−264.

(42) Riddick, J.; Bunger, A. Organic Solvents. In *Techniques of Chemistry*; Weissberger, A., Ed.; Wiley-Interscience; New York, 1986; Vol. II.

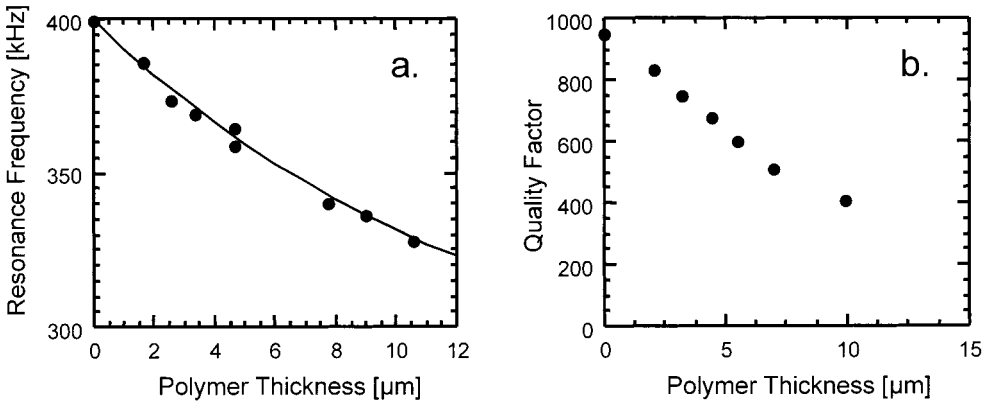

Figure 6. (a) Measured (●) and modeled (line) resonance frequency shift as a function of the polymer thickness (PEUT). (b) Quality factor of a cantilever as a function of the polymer thickness (PEUT).

Table 1. Measured Sensitivity of a Resonant Cantilever Coated with 2.4 μm of PEUT to Various Analytes at a Static Heating Power of ~10 mW[a]

analyte	sensitivity (Hz/ppm)	saturation vapor pressure (Pa)	mol wt
n-octane	−0.05	2200	114
toluene	-0.10	4300	92
ethyl acetate	-0.02	14400	88
ethanol	-0.01	8700	46

[a] Saturation vapor pressure at 301 K and molecular weight of the analytes are also listed.

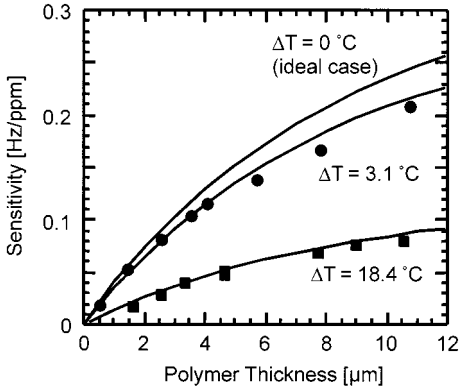

Figure 7. Measured (●) and modeled (solid lines) *n*-octane sensitivity versus polymer thickness for different cantilever temperatures. ΔT refers to ambient temperature (gas phase and sensor chip).

depend strongly on the homogeneity and morphology of the polymer film and, thus, on the quality of the deposited layer and the reproducibility of the deposition process.

Sensitivity and Limit of Detection. The sensitivity S of the gas sensor is the product of the thickness-independent analyte sensitivity, S_A, and a thickness-dependent gravimetric sensitivity *G*. The total sensitivity of the resonant beam gas sensor, *S*, consequently depends on the thickness of the applied polymer layer. To achieve experimental confirmation, cantilever sensors were coated with PEUT layers of varying thickness and were then exposed to various analytes.

The different slopes of the sensor response of a PEUT-coated cantilever upon analyte exposure are listed in Table 1. The sensor was coated with 2.4 μm of PEUT and actuated by ~10 mW heating power. Linear responses are to be expected in the low-concentration range (less than 1−2% of the saturation vapor pressure at the respective operation temperature), since Henry's law is valid. The long-term drift of the resonance frequency was subtracted from the measurements.[27] A frequency shift of 49 Hz was, for example, measured for 400 ppm toluene. The different analytes evoke different sensor responses as a consequence of their different molecular weights, their different gas-phase saturation vapor pressures, and the different partition coefficients of the analytes in PEUT. The response slope of, for example, toluene is considerably higher than that of ethanol, since toluene is less volatile (higher partitioning in PEUT), its molecular weight is higher, and its saturation vapor pressure is lower.

The gas-phase/polymer partitioning of the analyte is strongly dependent on the operation temperature. Since the cantilevers are thermally actuated, the relevant temperature in the polymer-coated sensing area of the cantilever might significantly deviate from the temperature of the surrounding chip and gas phase: The cantilever dissipates a static electrical power of 6 mW originating from the actuator and 1.25 mW from the piezoresistive Wheatstone bridge. The resulting temperature difference between cantilever and environment at routine operation was assessed to be 3.1 °C, which is in good agreement with modeling results. The increased cantilever temperature (heating resistors and piezoresistive Wheatstone bridge) affects the analyte partition coefficient, which depends in an exponential way on the temperature: the higher the temperature, the lower the partition coefficient and, hence, the lower the cantilever sensitivity. Figure 7 shows modeled and measured sensor sensitivity to *n*-octane as a function of the polymer (PEUT) thickness at two different cantilever temperatures. The two temperatures were achieved by variation of the static heating power applied to the heating resistors and by varying the power consumption of the Wheatstone bridge. The modeled sensitivity for the ideal case without any temperature increase on the cantilever is shown as well. Agreement between modeling and measurements is quite good since the discrepancy between measured and modeled sensitivities amounts to only 10−16%. Reasons for this discrepancy may include the uncertainty in the polymer thickness measurement or in the determination of the partition coefficients as well as CMOS process or material property fluctuations.

From the aforementioned considerations, it can be concluded that the partition coefficients assessed with cantilevers at a certain temperature are ∼20% lower than that determined with other mass-sensitive devices as a consequence of the slightly enhanced cantilever temperature (∼3 °C above ambient).

Cantilever sensitivity is also dependent on the polymer thickness. The sensitivity linearly increases with increasing layer thickness in the range of thin polymer layers (2−4 μm) and then shows a saturation-like behavior at larger thickness (>4 μm), as can be seen in Figure 7. The reason for this behavior is of mechanical nature and is not a consequence of the involved physicochemistry. At low polymer thickness, the mass increase upon gas absorption and the corresponding frequency shift are linearly correlated with the polymer thickness: The thicker the polymer, the more gas is absorbed, and the higher is the absolute frequency change. This does not hold for thicker polymer layers. Here, the fundamental resonance frequency, f_0, of the coated cantilever is considerably reduced as a consequence of the increased added mass by the thick polymer layer. The analyte-induced frequency shift (absolute value) upon gas exposure is also reduced due to the lower starting resonance frequency without analyte dosing. The sensor signal and hence the sensitivity are significantly lower than expected by linear extrapolation of the behavior at low polymer layer thickness. For a polymer thickness larger than 30 μm (not shown), the polymer elastic properties would prevail over those of the silicon oxide−nitride sandwich and then largely contribute to the sensor response (transition from a polymer-coated silicon cantilever to a silicon-coated polymer cantilever). At such large layer thickness, the sensitivity would again linearly increase with increasing polymer thickness (more polymer absorbs more analyte). Such behavior is in contrast to the results of Maute et al. (inflection point-like behavior[23]), where only the polymer mass is accounted for in the sensitivity behavior but not the polymer elastic properties.

The polymer thickness influences not only the sensitivity but also the short-term noise of the device. Optimization of the sensor aiming at a minimum detection limit hence includes not only sensitivity considerations but also a careful assessment of the sensor short-term stability and noise. The minimum detectable gas concentration, c_{min}, is usually defined as the gas concentration, the corresponding frequency shift, Δf_{min}, of which equals 3 times the short-term stability, Δf_n, of the sensor, in this case the cantilever resonator:

$$\Delta f_{min} = 3\Delta f_n \Rightarrow c_{min} = 3(\Delta f_n / S) \qquad (12)$$

Figure 8 shows the experimentally assessed resonator short-term stability or frequency noise, Δf, and the resulting detection limit, c_{min}, for octane and PEUT. For small PEUT thickness, the short-term stability is ∼0.03 Hz. It is limited by the noise of the oscillator circuit rather than the mechanical resonator properties. As the polymer thickness increases, the noise increases as well due to the polymer-induced reduction in quality factor of the resonator (see Figure 6b). For a thickness larger than 6 μm, the noise increase is rather drastic up to a value of ∼2.5 Hz at 10.7-μm layer thickness. The detection limit at small layer thickness is thus determined by the rather low sensitivity as a consequence of the small polymer volume. At large film thickness, the polymer-induced frequency stability reduction deteriorates the detection limit. Between 3- and 4-μm layer thickness, the detection limit c_{min} for octane passes an optimum. While the short-term stability is better for smaller thickness, the sensor sensitivity is lower, and this drawback outbalances the better frequency stability. For thicker polymer layers, the sensitivity is higher (more mass absorbed) but the resonator is less stable due to the reduced quality factor. With a frequency resolution of 0.03 Hz (counter gate time, 1 s) and a sensitivity of 0.12 Hz/ppm, a limit of detection of 0.8 ppm octane can be achieved at the optimum thickness of PEUT. The corresponding mass increase on the cantilever is 320 fg. Measurements were conducted down to concentrations of 5 ppm (Figure 9), which corresponds to a mass change of 2 pg.

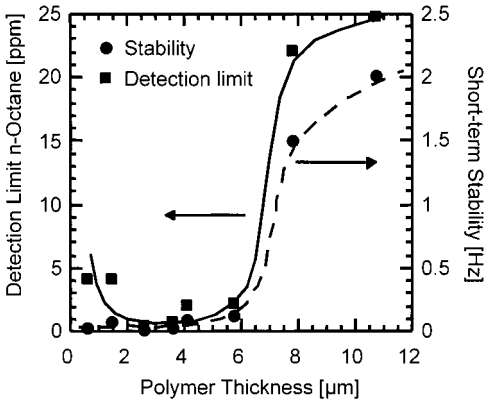

Figure 8. Short-term frequency stability and corresponding limit of detection of a PEUT-coated cantilever exposed to *n*-octane as a function of the polymer thickness. The lines are only guides to the eye.

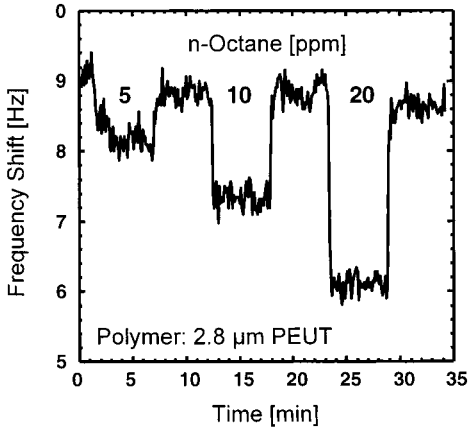

Figure 9. Low-concentration sensor responses: 5, 10, and 20 ppm *n*-octane dosed to a cantilever, which was coated with a 2.8-μm-thick PEUT layer.

However, applications may exist for which external noise is introduced to the sensor system such as temperature, gas flow fluctuations, or strong external electromagnetic fields. It is then advantageous to use thicker polymer layers, the reduced short-term frequency stability of which is less significant than the external noise introduced to the system.

QUANTITATIVE ANALYSIS USING CANTILEVER ARRAYS

Polymers as sensitive layers are only partially selective. A PEUT-coated sensor will respond to ethanol but also to many other

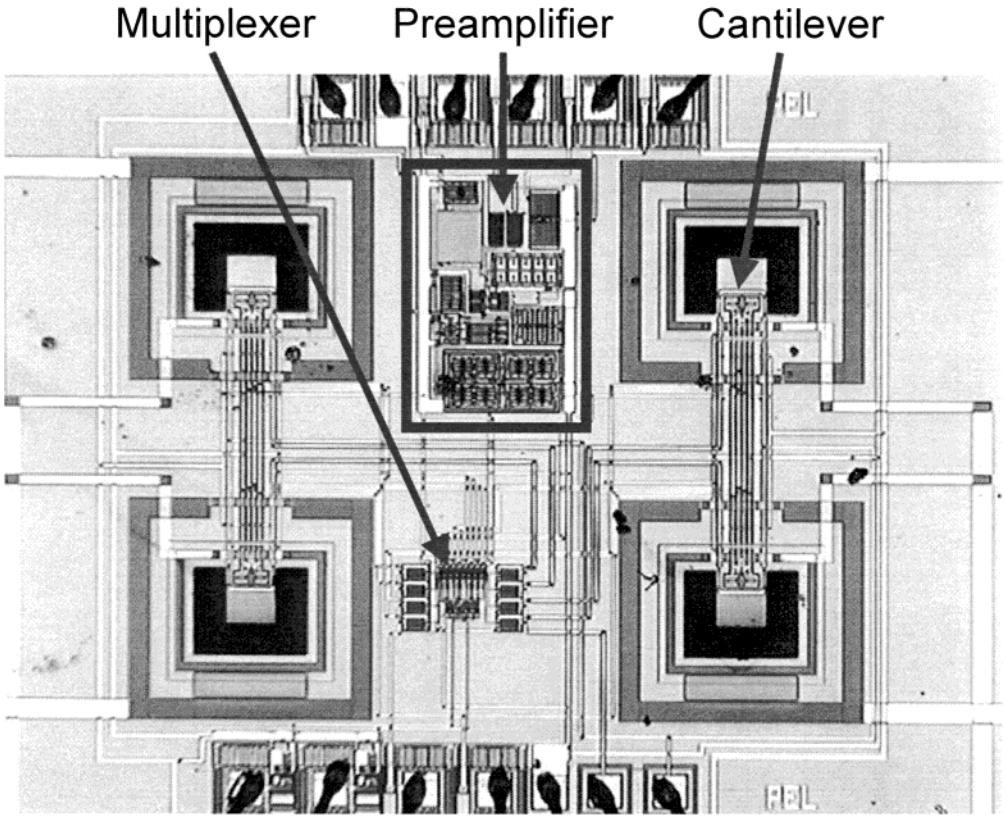

Figure 10. Micrograph of an integrated array of four cantilever gas sensors.

analytes with varying sensitivity. Better discrimination can be achieved with a system of more than one sensor, a so-called sensor array. Figure 10 shows a micrograph of an integrated cantilever array comprising four cantilevers, a preamplifier, and a multiplexer to sequentially address and operate the sensors. The resonance frequencies of the cantilevers are in the range of 380−410 kHz and differ by a maximum ±10%. The same holds for the quality factor of the resonators, which is 980 ± 10%.

To illustrate the use of cantilever arrays for quantitative analysis, a binary mixture of *n*-octane and toluene was dosed to the sensors. The analytes show different interaction and hence sorption properties. *n*-Octane is nonpolar and not polarizable, whereas toluene contains an aromatic ring with enhanced electron density, which renders the molecule polarizable. Measurements with mixtures of varying *n*-octane and toluene contents were recorded. Three cantilevers of the array were coated with 0.6 μm of PDMS, 1.5 μm of PCPMS, and 1.8 μm of PEUT. One cantilever was left uncoated to look into surface adsorption phenomena, which were found to be marginal. The signals of the uncoated cantilever were not included in the data evaluation.

The mixture analysis was performed in two steps. First, a calibration set was acquired by dosing mixtures with defined *n*-octane and toluene concentrations to the cantilevers. The calibration set comprised 28 data points with toluene concentrations between 300 and 700 ppm and *n*-octane concentrations between 200 and 700 ppm. The measured frequency shifts were normalized with regard to the maximum response value and divided by their standard deviation. This way, all sensors have the same weight in the prediction model. The standardized sensor responses serve as the input for the principal component analysis (PCA). For quantitative analysis a partial-least-squares (PLS) multilinear regression model was chosen.[43] More than 99% of the total information was found contained in the first two principal components. The sensor signals of the PDMS-coated sensors were closely correlated to the *n*-octane concentrations, whereas the PCPMS-coated sensor is rather sensitive to toluene. PEUT shows a considerable affinity to toluene as well. Though PEUT shows a larger partition coefficient of toluene than PCPMS, the PCPMS-coated sensor provides the dominating response for predicting toluene concentrations. This can be attributed to the fact that the PCPMS partition coefficient of toluene is 3.6 higher than that of *n*-octane. For PEUT, the toluene/*n*-octane partition coefficient ratio is only 1.3.

The model, which was developed using the calibration set, was then applied to predict a set of 16 independent test mixtures with unknown composition. The combinations of toluene and *n*-octane concentrations in the test set were chosen within the range covered by the calibration. The specific test compositions, however, were not contained in the calibration set. The quantitative results for the test set are shown in Figure 11a and b, respectively, for *n*-octane and toluene. The graphs show predicted versus true concentrations for both analytes. The ideal correlation is sketched as a straight line. The predicted values show a small positive offset; i.e., higher concentrations are predicted than were actually adjusted in the flow manifold. This can be explained by the fact that the strongly polar PCPMS forms droplets on the cantilever. Hence, the layer is not uniform and changes its morphology with increasing oscillation time (flows from strongly moving to less moving areas of the cantilever). This leads to a systematic signal

(43) Hierlemann, A.; Schweizer-Berberich, M.; Weimar, U.; Kraus, G.; Pfau, A.; Göpel, W. Multicomponent Analysis. In *Sensors Update*; Baltes, W., Göpel, J., Hesse, H., Eds.; Wiley-VCH: Weinheim, Germany, 1996; Vol. 2.

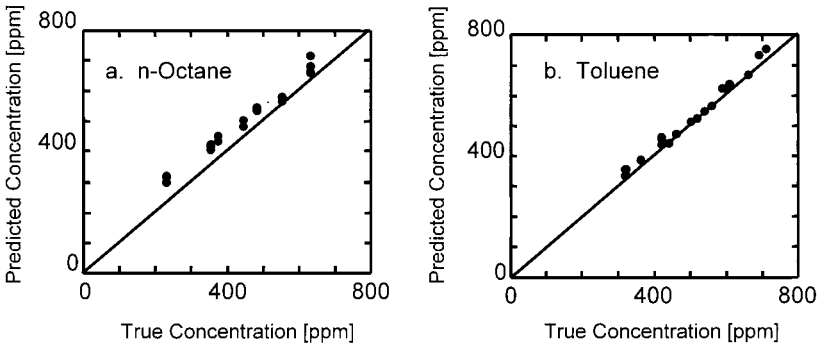

Figure 11. Predicted versus true concentration of *n*-octane (a) and toluene (b) in a binary mixture resulting from a partial least-squares regression.

divergence (offset) between calibration set and test set responses. Good correlation between the true concentration values and the predicted values was still achieved. In general, the toluene prediction was better, since the PDMS layer that dominates the *n*-octane prediction was relatively thin, which results in a smaller sensitivity and inferior resolution. These promising results establish the quantitative determination of components of a binary mixture with miniaturized mass-sensitive cantilevers.

COMPARISON TO OTHER ACOUSTIC GAS SENSORS

In this section, the sensing performance of the resonant cantilever will be compared with that of already established mass-sensitive transducers. Presently, TSMR and Rayleigh SAW devices are the most common devices to monitor volatile organic compounds.[15−18] The sensitivity equations for cantilevers and TSMRs are very similar. The cantilever eq 11 can be rewritten by replacing the cantilever mass density (only cantilever sandwich materials), ρ_{cant}, for ρ_{mean}, to separate layer and transducer variables:

$$S = -\frac{1}{2\left(\rho_{cant} + \rho_L \frac{t_L}{t_{cant}}\right)} \frac{t_L}{t_{cant}} f_0 K_c \qquad (13)$$

The corresponding equation for the TSMR can be derived from the Sauerbrey equation:[44]

$$S = -\frac{1}{\rho_{quartz}} \frac{t_L}{t_{quartz}} f_0 K_c \qquad (14)$$

A somewhat different equation could be derived for the Rayleigh SAW provided there are no modulus contributions to the sensor response.[45,46] The TSMR resonates in the thickness shear mode, and the polymer layer is not deformed through the transducer movement. In the case of the SAW devices, the polymer layer undergoes deformation and modulus terms must be accounted for as soon as the polymer modulus is beyond a certain limit.[47] More details of this modulus discussion can be found in refs 47 and 48. The cantilever vibration generally deforms the polymer, and therefore, modulus contributions have to be considered and are included in our equations. Due to the large spring constant of the cantilever materials (very stiff cantilever), we felt, however, justified to neglect the effect of sorption-induced polymer modulus changes (see eq 6) on the sensor response. This is further supported by the facts that all used polymers are low-modulus polymers and the analyte concentrations are very low.

A possibility to effectively exclude polymer contributions to the cantilever oscillation behavior is to coat only the cantilever tip and not the base, which experiences the maximum deformation.[26,49]

In comparing the two eqs 13 and 14, it is obvious that they comprise similar terms. The sensitivity is in both cases proportional to the fundamental device frequency, the partition coefficient, and the ratio of polymer layer thickness and transducer thickness. The main difference is that the TSMR equation (eq 14) does not have any term that is related to the mass density of the polymer layer. This can be explained by the fact that the Sauerbrey equation only describes simple mass loading. The use of a sensitive layer or sorption matrix is not included in the model used to derive the Sauerbrey equation. Additionally, it has to be noted that eq 14 only holds true for acoustically thin layers;[47] i.e., the polymer layers are thin enough that no phase lag between the moving quartz surface and the outer surface of the polymer coating occurs.[47,48] Otherwise, polymer modulus terms definitely have to be taken into account and the Sauerbrey equation has to be modified.

In the following, the cantilever results will be benchmarked against TSMR and SAW device results. Many authors of cantilever papers do report on or extrapolate to exceptional mass-sensitivity values of cantilevers. We do not completely share this enthusiasm. First one has to clearly distinguish between absolute mass sensitivity of the device and the gas sensor sensitivity based on analyte absorption. The absolute mass resolution of the cantilevers surely is in the range of a few picograms as assessed by many authors for different cantilever geometries and operation modes (static or dynamic).[5−13,19−24] However, this high absolute mass sensitivity does not necessarily imply an exceptionally high gas sensor sensitivity, since the area coated with the sensitive layer usually is very small (on the order of 100 × 150 or 100 × 500

(44) Sauerbrey, G. *Z. Phys.* **1959**, *155*, 206−222.
(45) Wohltjen, H. *Sens. Actuators* **1984**, *5*, 307−325.
(46) Ballantine, D. S.; Wohltjen, H. *Anal. Chem.* **1989**, *61*, 705−712.
(47) Martin, S. J.; Frye, G. C.; Senturia, S. D. *Anal. Chem.*, **1994**, *66*, 2201.
(48) Hierlemann, A.; Zellers, E. T.; Ricco, A. J. *Anal. Chem.* **2001**, *73*, 3458−3466.
(49) Thundat, T.; Maya, L. *Surf. Sci.* **1999**, *430*, L546−552.

Table 2. Comparison of Mass-Sensitive Sensors in Detecting 100 ppm *n*-Octane[a]

device	f_0 (MHz)	Δf_{poly} (kHz)	Δf_{gas} (Hz)	$\Delta f_{gas}/f_0 \times 10^6$	$\Delta f/\Delta T$ (Hz/K)	$\Delta f_{gas}/(\Delta f/\Delta T)$ (K)	LOD (ppm) S/N = 3
cantilever (301 K)	0.4	−35 (4 μm)	12.0	30	17	0.7	2.5
TSMR (303 K)	30	−71.6 (0.32 μm)	20.6	0.7	−15	1.4	1.5
SAW delay line (303 K)	80	−330 (1.56 μm)	87.9	1	−160	0.6	7

[a] The frequency noise (short-term) was set to 0.1 Hz for the cantilever and the TSMR[17] and to 2 Hz for the SAW device[17] in determining the LODs.

μm). As a consequence, the overall polymer volume, which absorbs the analyte, and the resulting overall mass change upon analyte absorption on the cantilever is much less than for the larger TSMR and SAW devices. The better absolute mass sensitivity (or "resolution") of the cantilever is therefore counteracted by the small transducer dimensions.

Bodenhöfer et al. compared the sensing properties of polymer-coated TSMR and SAW devices.[17] Devices under investigation included a 30-MHz TSMR device (discrete piezoelectric quartz crystal, AT-cut, gold electrodes; Kristallverarbeitung Neckarbischofsheim) and an 80-MHz SAW delay line device (dual delay lines, quartz, aluminum electrodes, ST-cut; Xensor Integration). Both transducers were coated with PEUT up to the maximum thickness before oscillation was quenched (~320 nm for the TSMR and 1.56 μm for the SAW device). The gas manifold was similar to the one used in this paper. The measurement temperature was 303 K instead of the 301 K used here in the cantilever investigation. However, the cantilever temperature is ~3 °C higher than gas-phase and ambient temperature (thermal actuation), so that the polymer partitioning is more or less directly comparable for cantilevers and the TSMR or SAW devices reported in ref 17. The enhanced cantilever temperature as a consequence of the actuation scheme has to be kept in mind in assessing sensor device performances.

Table 2 includes characteristic experimental results for TSMRs and SAWs as taken from ref 17 and the cantilever data compiled in this study. Although the fundamental resonance frequency of the cantilever is more than 2 orders of magnitude lower than that of the other devices, its performance is comparable to those of TSMR and SAW delay line. Using a rather conservative frequency noise estimate of 0.1 Hz for the cantilever and TSMR as reported in ref 17 (in both cases, the measured short-term frequency noise is considerably lower; see ref 17), the limit of detection of the cantilever is 2.8 ppm *n*-octane (operation at 301 K ambient temperature), which is close to that of the TSMR (1.5 ppm) and better than that of the SAW delay line (7 ppm *n*-octane). Baller et al. extrapolated to sub-ppm level detection of propanol and other alcohols using rather long (length, 500 μm; width, 100 μm) and soft (thickness, 1 μm; spring constant, 0.02 N/m) cantilevers, which were coated with various polymers and operated in deflection mode (optical readout by means of a laser) and dynamic mode (piezoelectric actuation of the whole chip bearing the cantilevers, optical readout).[7,50,51] Boisen et al.[6] and Jesenius et al.[13] reported on a detection limit below 10 ppm ethanol for 200-μm-long, 50-μm-wide, and 2-μm-thick cantilevers operated in the deflection mode with piezoresistive readout. In both cases, syringe-based vaporization techniques at room temperature are used, which inherently do not allow a precise concentration adjustment. The detection of mercury at ppb levels using a gold-coated cantilever was reported.[29] This is, however, a different story since the extremely heavy mercury amalgamates into the gold, and the cantilever acts as a dosimeter. The absolute mass sensitivity of this device is on the same order of magnitude (0.7 pg/Hz)[29] as reported in this paper. From all these results, it looks like limits of detection (LODs) achieved with cantilevers are very similar to those obtained by TSMRs. Some differences in the transducer mechanics and characteristics, however, merit further discussion.

The large fractional frequency shift upon gas exposure as compared to the fundamental resonance frequency significantly contributes to the good performance of the cantilever. A cantilever beam shows an ~30 times higher fractional frequency shift than TSMRs and SAWs. The absolute frequency shift values of the cantilever are lower than that of the other devices, and therefore, frequency counters with higher precision are required for readout. On the other hand, it is not necessary to meet the strict high-frequency requirements (shielding, etc.) of SAW device operation.

The cantilever transducer also tolerates larger coating thicknesses, e.g., 4-μm coating thickness at 6-μm cantilever thickness (data in Table 2). This positively affects the transducer sensitivity as can be taken from the second term in eqs 13 and 14. In the case of the TSMR, the quartz plate thickness is 56 μm at 30 MHz, and the coating thickness is 100−300 nm. The thickness of SAW coatings is in the range of 200 nm to 1 μm; the thickness of the quartz plate (~1 mm), however, does not affect the device characteristics, since the penetration depth of the acoustic wave is approximately one wavelength (40 μm at 80 MHz, 7.3 μm at 433 MHz).

Both sensors (TSMR and cantilever) show a sensitivity proportional to the resonance frequency, as can be seen in eqs 13 and 14. However, in the case of the cantilever, the inherent geometry dependence (width, length, thickness) provides much more flexibility in optimizing sensor sensitivity. It is, for example, possible to increase the mass sensitivity by reducing the cantilever thickness. At the same time, a high cantilever resonance frequency can be maintained by shortening the cantilever. In contrast, the only parameter of a TSMR that can be tuned is its plate thickness.

(50) Baller, M.; Lang, H. P.; Fritz, J.; Gerber, C.; Gimzewski, J. K.; Drechsler, U.; Rothuizen, H.; Despont, M.; Vettiger, P.; Battiston, F.; Ramseyer, J. P.; Fornaro, P.; Meyer, E.; Güntherodt, H. J. *Ultramicroscopy* **2000**, *82*, 1−9.
(51) Battiston, F.; Ramseyer, J. P.; Lang, H. P.; Baller, M.; Gerber C.; Gimzewski, J. K.; Meyer, E.; Güntherodt, H. J. *Sens. Actuators, B* **2001**, *77*, 122−131.

Considering the temperature stability, the quartz is still preferable, whereas the cantilever shows a temperature dependence similar to that of the SAW device. This is a consequence of temperature-induced variation of material properties of the CMOS composite cantilever and the temperature-induced changes in the relatively thick polymer layer.

A last big advantage of the cantilever is its compatibility to microelectronics and the possibility to co-integrate transducer and electronics on a single chip (miniaturization). Placing all the oscillator circuitry, the amplifiers, and the analog/digital converter in the immediate vicinity of the transducer (Figure 1) drastically increases the overall device performance (better signal-to-noise ratio) and renders the chip less sensitive to external disturbances. The integrated feedback in particular eliminates cross-talk (capacitive, inductive) between the connections supplying the large heating currents for thermal actuation and the lines transmitting the small signals of the piezoelectric Wheatstone-bridge. Integration also simplifies the packaging because there are no sensitive analog signals that need to be shielded from external noise sources or electromagnetic interference, and integration allows for fabricating sensor arrays without increasing the number of bond wires by using an on-chip bus system (eight bond wires per sensor without on-chip electronics). Co-integration of circuitry furthermore enables the realization of "smart" and self-test features.

In summary, the resonant cantilever sensor discussed in this paper is a very compact gas-sensing system capable of detecting gas-phase concentrations of, for example, *n*-octane or toluene in the single-ppm range. The fabrication in industrial CMOS technology allows for the integration of transducers, driving circuitry, and analog or digital signal-processing circuitry on the same chip.[52] Integrated thermal excitation and piezoresistive detection schemes render the system independent of additional excitation elements such as piezoelectric layers[19] and independent of bulky external optical detectors.[7−9] The cantilever sensing behavior can be well described by an analytical model, which makes further improvements in sensitivity and limit of detection possible. The optimum polymer layer thickness was found to be 3−4 μm. Direct comparison to TSMR and SAW devices shows that resonant cantilevers exhibit comparable and partly better performance in terms of LOD and thermal stability. Resonant cantilever sensors operate at comparably low frequency, and therefore, the circuitry requirements are less stringent than the high-frequency requirements of Rayleigh SAW devices. In comparison to TSMRs, the resonant cantilevers offer the advantage of co-integration of signal conditioning and processing circuitry which enables the development of very compact arrays.

(52) Hagleitner, C.; Hierlemann, A.; Lange, D.; Kummer, A.; Kerness, N.; Brand, O.; Baltes, H. *Nature* **2001**, *414*, 293−296.

ACKNOWLEDGMENT

The authors are greatly indebted to former staff of the Physical Electronics Laboratory at ETH Zurich involved in the chemical microsensor development. The services of the prototype manufacturers Austriamicroystems Int. (Unterpremstäten, Austria) are gratefully acknowledged. Low-concentration measurements were performed with the manifolds of the University of Tübingen (Dr. U. Weimar). The project was financially supported by the Körber Foundation (Hamburg, Germany).

Received for review December 19, 2001. Accepted March 15, 2002.

AC011269J